



Shift Register for Graphene Kinks

Dyk Chung Nguyen and Yuriy V. Pershin *

Department of Physics and Astronomy, University of South Carolina, Columbia, South Carolina 29208, USA

 (Received 26 January 2022; revised 11 May 2022; accepted 10 August 2022; published 1 September 2022)

Recently, there have been many developments in domain-wall electronics, such as racetrack memory and domain-wall logic. Here, we show that some of the principles of the control of ferromagnetic and ferroelectric domain walls can be applied to graphene kinks and antikinks, which are topological states of buckled graphene membranes. Using molecular-dynamics simulations, we demonstrate the good properties of graphene kinks for application in a racetracklike memory. Specifically, it is shown that in a sawtooth (ratchetlike) potential, graphene kinks and antikinks are locked into discrete positions on the membrane, and their force-induced unidirectional motion resembles the operation of a digital shift register.

DOI: [10.1103/PhysRevApplied.18.034002](https://doi.org/10.1103/PhysRevApplied.18.034002)

I. INTRODUCTION

Racetrack memory is a promising nonvolatile memory technology introduced by Parkin *et al.* in 2008 [1,2]. In racetrack memory, a spin-coherent electric current pushes a sequence of magnetic domains along ferromagnetic nanowires, and this sequence is read or modified by stationary read and write heads. In 2012, Franken *et al.* [3] introduced a different realization of racetrack memory, in which the domain walls are localized at discrete locations with the help of a ratchetlike energy landscape and moved by magnetic field pulses. Importantly, the interplay of the magnetic field and the ratchetlike potential causes unidirectional motion of the domain walls (under appropriate conditions). A few years later, a ferroelectric shift register was demonstrated by White and Gregg [4]. In their experiments, a sawtooth energy landscape was introduced by variation of the material thickness, while ferroelectric domains were driven by a transverse electric field. Some other approaches to ferromagnetic shift registers have been reported in the literature [5,6].

In fact, the concept of racetrack memory or shift registers can be extended further to very different experimental systems, albeit in a modified form. In particular, in the present paper we demonstrate that the approach of Franken *et al.* [3] can be applied to graphene kinks and antikinks [7]. Graphene kinks and antikinks are topological states of long graphene membranes buckled in the transverse direction [7]. Such states may not be unique to graphene, but single- or double-layer graphene seems to be the simplest experimental platform for their realization. Only theoretical studies of graphene kinks have been reported so far [7–9]. These studies have demonstrated the rich physics

of topological states in buckled graphene, including their connection to the classical ϕ^4 field-theory model [7], a negative-radiation-pressure effect [8], and resonances in the scattering of kinks by a constriction [9]. Some relevant studies of the classical ϕ^4 model are Refs. [10–18].

It should be mentioned that graphene kinks [7] are more complex than the classical ϕ^4 kinks [18]. This is a direct consequence of the two-dimensional nature of long graphene membranes, in which the longitudinal degrees of freedom are “dressed” by the transverse degrees of freedom. There exist two types of graphene kinks and antikinks, α and β . In α (β) kinks, the central transverse cross section has two (one) zero crossings [19]. The sign \pm in the notation for kinks [19] represents the sign of the transverse cross section of the kink or antikink. For instance, the membrane deflection close to the kink or antikink center in an (α, \pm) kink or antikink behaves as $z(x \approx x_0, y) \propto \pm \cos(3\pi y/d)$, where x_0 is the position of the kink and d is the width of the membrane. Readers may wish to refer to Ref. [19], where the classification of graphene kinks is introduced in detail.

A conceptual image of a shift register is presented in Fig. 1. Here, a graphene membrane is positioned above a trench in an insulating substrate, and buckled in the transverse (z) direction. The trench has a modulated (sawtooth) width, causing a ratchetlike potential for graphene kinks and antikinks. Several metal electrodes are positioned in the vicinity of the membrane to actuate the membrane and read its state. The actuation uses the electrostatic force between two oppositely charged electrodes. The electrodes shown above the membrane represent read and write heads. For the shift operation, a force is applied homogeneously to all atoms of the membrane. To create a kink or antikink, a force is applied locally using a local electrode (see Ref. [7], where the same method was used

*pershin@physics.sc.edu

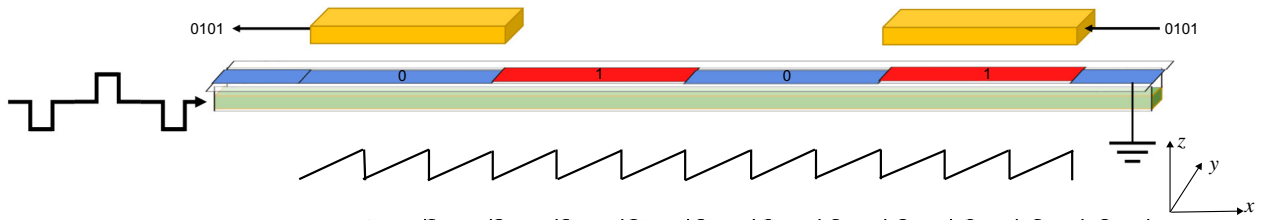


FIG. 1. Conceptual schematic illustration of a shift register for graphene kinks. Here, a buckled graphene membrane is positioned above a trench (the trench is in the x direction). The data is encoded in the direction of membrane buckling. The regions where the membrane is buckled up (red) correspond to one (1), and the regions where it is buckled down (blue) to zero (0). Metal electrodes located in the vicinity of the membrane are used for the purposes of shift control and of reading and writing. The sawtooth curve shown at the bottom represents the shape of the trench edge (the other edge has a symmetric shape). The edge is shown as viewed from the top (in the x - y plane).

to create kinks). The state of the membrane can be read locally by measuring the capacitance between the membrane and an electrode. The use of a ratchetlike potential is inspired by Ref. [3]. The ratchetlike potential breaks the symmetry along the membrane, and results in unidirectional motion of kinks and antikinks under appropriate driving conditions.

This paper is organized as follows. In Sec. II, we introduce the details of the molecular-dynamics simulations that we perform. In Sec. III, it is shown that in the presence of a sawtooth potential, the topological states of the membrane are localized at discrete locations. In this demonstration, we simulate the dynamics of graphene kinks and antikinks starting from different initial positions, and observe their drift and their localization in regions where the trench is narrower. Thereafter, we investigate the manipulation of individual kinks by a homogeneous force in the vertical direction, and the integration of individual shifts into the operation of a shift register. Finally, the paper ends with a discussion and conclusion (Sec. IV).

II. SIMULATION DETAILS

Molecular-dynamics simulations are performed using the NAMD package [20]. VMD [21] is used for visualization of the atomic coordinates [22]. The interactions between the carbon atoms in the graphene are described using parameters of CA-type atoms in a CHARMM27 force field [23,24]. The potential function includes bond-length, bond-angle (including the Urey-Bradley term), dihedral-angle, and Lennard-Jones potential-energy terms.

As a starting point, we define a flat graphene nanoribbon of length 1400 Å and width 31 Å. The nanoribbon is compressed by 10% in the y direction. The attachment to the substrate is taken into account by fixing the atoms along the two long edges in a sawtooth fashion with a period of 100 Å and an amplitude of 5 Å (see the orange curves in Fig. 2). The membrane is buckled by applying a small force in the z direction to all atoms for 5000 steps, followed by energy minimization for 10^4 steps under zero force.

Our simulations are performed using Langevin dynamics at $T = 293$ K with a damping parameter of 0.5 ps^{-1} . We use a time step of 1 fs. The van der Waals interactions are truncated at a cutoff distance of 12 Å, with the “switchdist” parameter set to 10 Å. The electrostatic interaction between the metal electrodes and the membrane is taken into account by means of external forces applied to the membrane atoms. The position of the kinks and antikinks is determined by finding the crossings of the $z = 0$ plane with the chain of atoms at the center of the membrane ($y = 0$). In simulations of the entire register, we use a homogeneous force in the x direction in each shift phase to fix the type of kinks and antikinks.

III. RESULTS

A. Equilibrium positions

As a first step in this study, we identify equilibrium positions for kinks and antikinks along the membrane. Here and in what follows, we focus on α -type kinks and antikinks, as β kinks and antikinks are less stable and can not be easily created. In particular, the creation of β kinks or antikinks would require the application of a force asymmetric in the y direction—something that cannot be achieved in the setup under consideration (Fig. 1).

To define the initial geometry, a force in the vertical (z) direction is applied to a group of atoms near the right or left edge of the membrane. Under certain conditions, this force creates a kink or antikink moving at a velocity determined by the magnitude of the force [7]. Using different evolution times, we manage to position (α, \pm) kinks and antikinks at desired locations along the membrane. The final geometry of the membrane found here is used as the initial state in the following calculations.

Using comprehensive MD simulations, we identify stable and unstable equilibrium points for graphene kinks and antikinks. Figure 2 shows the most important results of these simulations. Here, we plot the total potential energy as a function of the position of a kink or antikink as the kink or antikink moves from the vicinity of an unstable

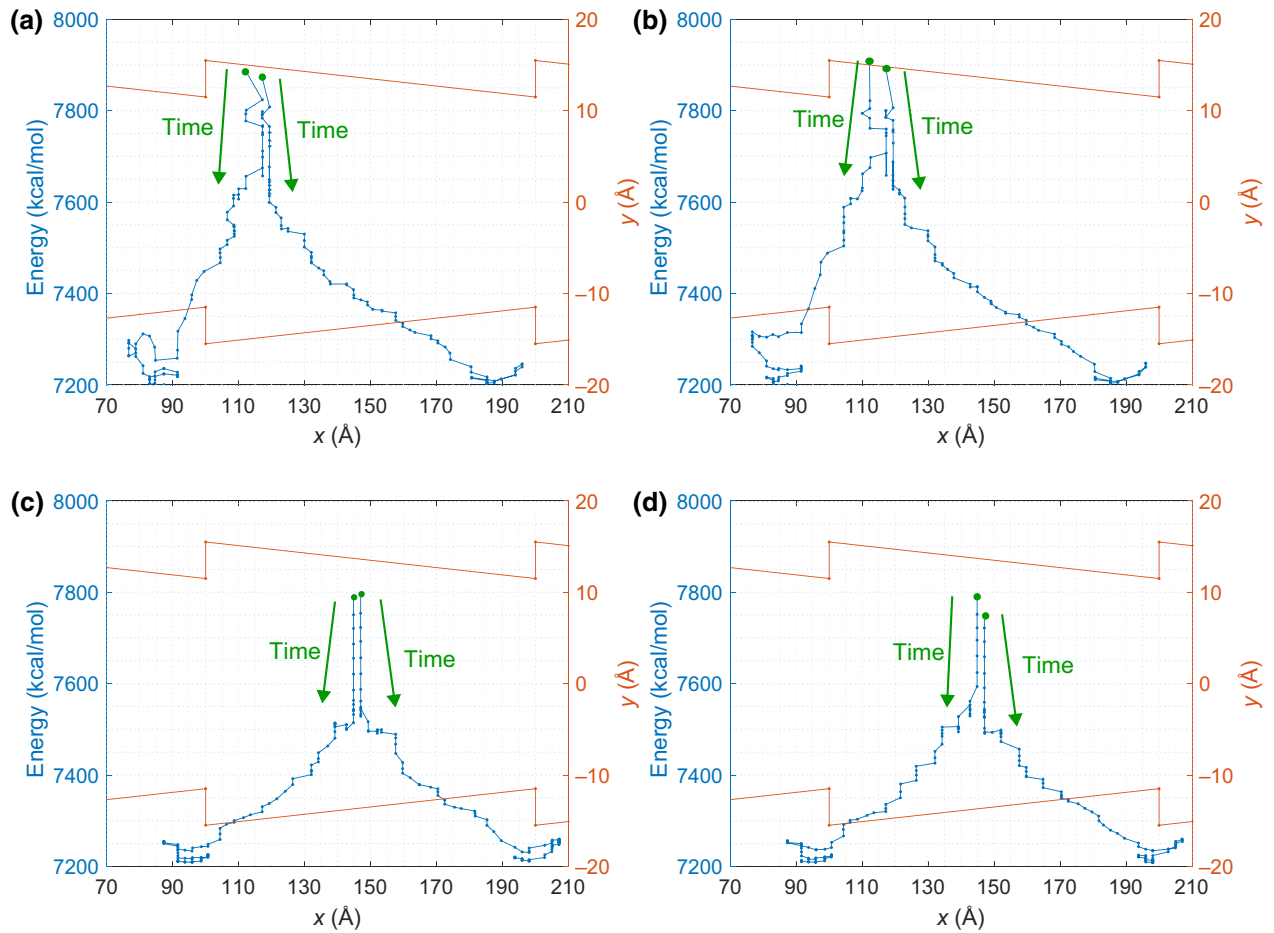


FIG. 2. Equilibrium positions of (a) $(\alpha, -)$ antikink, (b) $(\alpha, +)$ kink, (c) $(\alpha, +)$ antikink, and (d) $(\alpha, -)$ kink. These plots show the energy as a function of position as the kink or antikink moves to its equilibrium position. Two trajectories starting very close to an unstable equilibrium point are shown in each plot. The orange curves made of line segments represent the trench shape as viewed from the top.

equilibrium point to a stable equilibrium point. According to Fig. 2, the unstable equilibrium points for $(\alpha, +)$ antikinks and $(\alpha, -)$ kinks are located close to the middle of the interval where the sawtooth profile ramps [see Figs. 2(c) and 2(d)]. The unstable equilibrium points for $(\alpha, -)$ antikinks and $(\alpha, +)$ kinks are shifted to wider regions of the trench [see Figs. 2(a) and 2(b)]. The difference in the locations of the stable equilibrium points is smaller. For all types of kinks and antikinks, the stable equilibrium points are located where the trench is narrower.

Overall, Fig. 2 demonstrates that the sawtooth shape of the trench creates favorable discrete locations for kinks and antikinks. In the absence of external forces, the graphene kinks and antikinks are localized at these locations.

B. Unidirectional shift

It is not difficult to realize that a vertical force applied to a membrane fixed homogeneously pushes kinks and

antikinks in opposite directions. Obviously, the sawtooth potential introduces asymmetry into the motion of kinks and antikinks, as it sets up different potential gradients for motion to the right and to the left. This asymmetry is essential for the operation of our shift register. In this section, we first demonstrate that under appropriate conditions, kinks and antikinks can be shifted unidirectionally by mechanical force pulses.

Consider a buckled graphene membrane with a single kink or antikink, initially positioned in the vicinity of a stable equilibrium point. The membrane is subjected to a sequence of alternating force pulses in the $+z$ and $-z$ directions. The force is applied to the membrane homogeneously; namely, the same force is applied to each atom. Using a trial-and-error strategy, we identify the parameters of the pulse sequence such that the kink or antikink is shifted in each period of the pulse sequence by one period of the sawtooth potential (100 Å). Figure 3 exhibits selected results of these simulations.

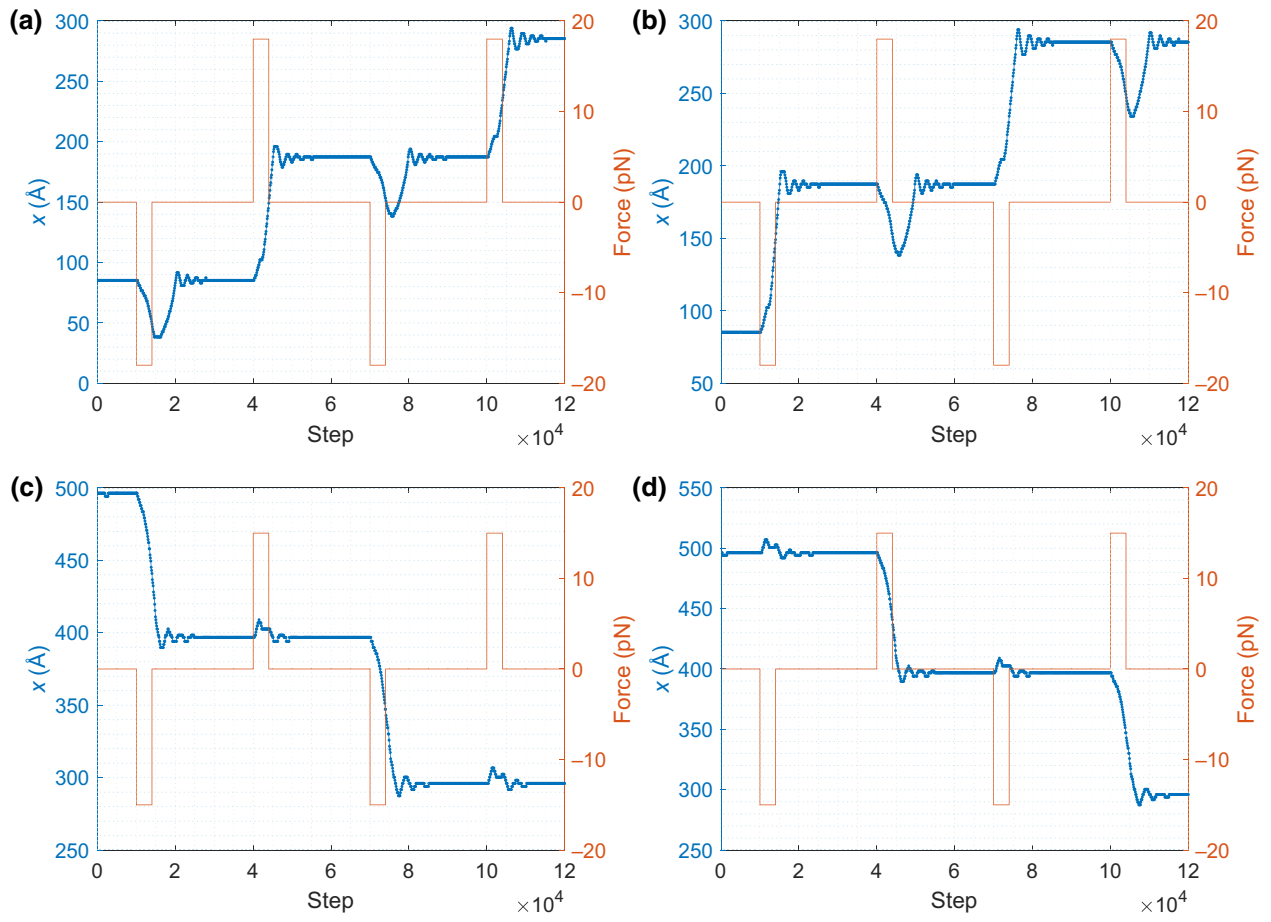


FIG. 3. Dynamics of kinks and antikinks induced by force pulses: (a) $(\alpha, -)$ antikink, (b) $(\alpha, +)$ kink, (c) $(\alpha, +)$ antikink, and (d) $(\alpha, -)$ kink. In these simulations, the force pulses are applied in the z direction homogeneously to all membrane atoms. The force magnitude is given per atom.

It is interesting that the graphene kinks and antikinks can be separated into two groups depending on the minimum magnitude of the force required for their shift, and their shift direction. The first group consists of $(\alpha, -)$ antikinks and $(\alpha, +)$ kinks, which require a force of approximately 18 pN and shift in the positive x direction. The second group comprises $(\alpha, +)$ antikinks and $(\alpha, -)$ kinks, which shift in the negative x direction, and the required force magnitude for them is approximately 15 pN.

Clearly, in a shift register, 0s and 1s must be shifted in the same direction. To achieve this objective, one can combine either $(\alpha, -)$ antikinks and $(\alpha, +)$ kinks or $(\alpha, +)$ antikinks and $(\alpha, -)$ kinks in the same system [25]. Additionally, to avoid loss of information, the interaction between individual kinks or antikinks, as well as their interaction with noise (introduced by the force pulses), needs to be sufficiently small. In our molecular-dynamics simulations, we find that binary information is stored reliably when one bit of information is encoded in three periods of the sawtooth potential.

Simulations of an entire shift register are presented in Fig. 4. This plot shows the sequence of changes caused by force pulses applied to a membrane with $(\alpha, +)$ antikinks and $(\alpha, -)$ kinks initially positioned as shown in Fig. 4(a). To shift the information to the left, we first apply a -15 -pN force pulse in the z direction for 4000 steps, followed by an equilibration period. During this period, noise and oscillations are reduced because of damping. The final state of the membrane is shown in Fig. 4(b). Next, we apply a $+15$ -pN force pulse, which completes the shift of all kinks and antikinks by one position of the potential to the left [Fig. 4(c)]. Next, we repeat everything two more times, since three periods of the sawtooth potential are used per bit. Figure 4(d) presents the final state of the membrane, showing a binary shift by one to the left.

IV. DISCUSSION AND CONCLUSION

In this paper, we propose a racetracklike device—a shift register for graphene kinks and antikinks—and explore computationally several aspects of its operation. Our

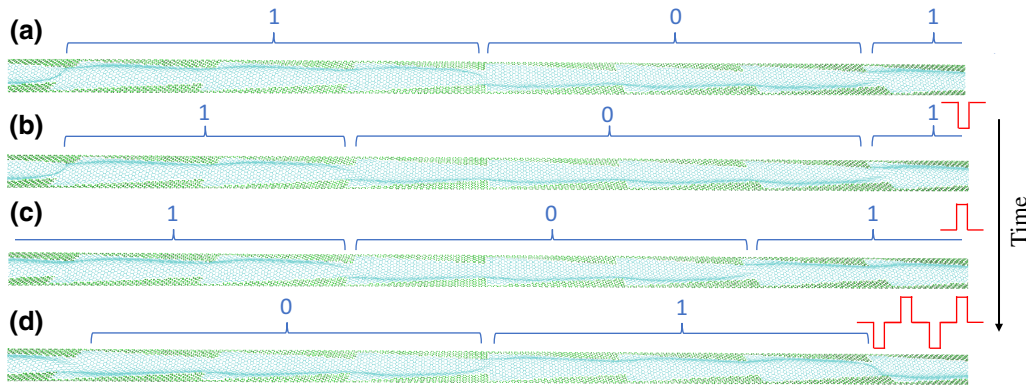


FIG. 4. Shift of information induced by force pulses (the z component of the force is shown schematically in red). (a) Initial state of the membrane, 0101 (for the sake of clarity, this figure shows only the central part of the membrane, corresponding to the central bits 10 in 0101). (b) Nanoribbon after 30 000 simulation steps. Notice that a downward force pulse shifts antikinks by one period to the left. (c) An upward force pulse shifts kinks by one period to the left. (d) A sequence of four alternating force pulses shifts all kinks and antikinks by two periods to the left.

results indicate that in the presence of a sawtooth potential, a sequence of 0s and 1s can be stored reliably in the membrane state. Moreover, when the transitional regions between the bits are implemented by specific pairs of kinks and antikinks, external force pulses can be used to shift information unidirectionally along the membrane.

From the point of view of fabrication, it is feasible to create the proposed shift register using conventional processes for the manipulation of graphene and for the fabrication of microelectromechanical and nanoelectromechanical systems. These processes have been used to make various graphene-based nanoelectromechanical switches [26–28] and thermal switches [29]. The actuation in these devices is caused by electrostatic forces between oppositely charged graphene and fixed metal electrodes [30] (the same method is employed in our device). Perhaps the most challenging aspect will be to implement the buckling. For this purpose, one can potentially utilize the negative thermal expansion of graphene [31,32]: if it is transferred to a surface at a high temperature, the graphene will then cool, expand, and buckle. Another possibility is based on the use of a polymer sacrificial spacer [27]. If the graphene is transferred to a curved polymer surface bounded by supports, the graphene will stay buckled after the polymer spacer is dissolved.

Despite being introduced more than a decade ago [1], racetrack-memory technology has not been yet demonstrated on a large scale. Therefore, it is of interest to consider alternative approaches, even if from only an academic point of view. The shift register proposed here has several merits. First, it employs the solid-state analogs of topological states in the classical φ^4 theory—kinks and antikinks—whose motion in graphene is characterized by low energy dissipation [7] (the classical kinks and antikinks are dissipationless [18]). Second, the propagation

speed of these states can be as high as 5 km/s [7], compared with the speed of domain walls of approximately 1 km/s in the latest Racetrack Memory 4.0 [2]. Third, the write energy per bit can be estimated as a few times the energy of a kink. Using 300 kcal/mol as the kink energy [7], we arrive at 10^{-17} J/bit. This energy is significantly smaller than the write energy per bit in other emerging memory devices and comparable only to the write energy in DNA massive storage devices [33]. Last but not least, micromechanical systems have attracted a lot of interest because of the possibility of using them in the quantum regime [34]. Therefore, we expect that our proposal may lead to the development of a *quantum shift register*, which may become a memory component in future quantum computers.

We emphasize that the present paper sets out the theoretical foundation for a kink-based shift register, focusing on the mechanics of its operation. To make the analysis manageable, we abstract from certain details of the setup shown in Fig. 1, such as the details of the electrostatic interaction, assuming, in particular, that the forces that are considered can be exerted in practice. From an experimental point of view, it may be technologically challenging to manufacture a shift register for graphene kinks today. Moreover, defects and variations in the structure and applied forces may influence the robustness of the proposed device. However, a detailed study of these effects is beyond the scope of our work, although it should be addressed in the future. In any case, we believe that these results will be useful, in one way or another, in the development of next-generation memories.

[1] S. S. Parkin, M. Hayashi, and L. Thomas, Magnetic domain-wall racetrack memory, *Science* **320**, 190 (2008).

- [2] S. Parkin and S.-H. Yang, Memory on the racetrack, *Nat. Nanotechnol.* **10**, 195 (2015).
- [3] J. Franken, H. Swagten, and B. Koopmans, Shift registers based on magnetic domain wall ratchets with perpendicular anisotropy, *Nat. Nanotechnol.* **7**, 499 (2012).
- [4] J. Whyte and J. Gregg, A diode for ferroelectric domain-wall motion, *Nat. Commun.* **6**, 1 (2015).
- [5] D. Allwood, G. Xiong, M. Cooke, C. Faulkner, D. Atkinson, N. Vernier, and R. Cowburn, Submicrometer ferro-magnetic NOT gate and shift register, *Science* **296**, 2003 (2002).
- [6] D. A. Allwood, G. Xiong, C. Faulkner, D. Atkinson, D. Petit, and R. Cowburn, Magnetic domain-wall logic, *Science* **309**, 1688 (2005).
- [7] R. D. Yamaletdinov, V. A. Slipko, and Y. V. Pershin, Kinks and antikinks of buckled graphene: A testing ground for the ϕ^4 field model, *Phys. Rev. B* **96**, 094306 (2017).
- [8] R. D. Yamaletdinov, T. Romańczukiewicz, and Y. V. Pershin, Manipulating graphene kinks through positive and negative radiation pressure effects, *Carbon* **141**, 253 (2019).
- [9] D. C. Nguyen, R. D. Yamaletdinov, and Y. V. Pershin, Influence of a constriction on the motion of graphene kinks, *Phys. Rev. B* **103**, 224312 (2021).
- [10] J. A. Combs and S. Yip, Single-kink dynamics in a one-dimensional atomic chain: A nonlinear atomistic theory and numerical simulation, *Phys. Rev. B* **28**, 6873 (1983).
- [11] D. K. Campbell, J. F. Schonfeld, and C. A. Wingate, Resonance structure in kink-antikink interactions in ϕ^4 theory, *Phys. D: Nonlinear Phenom.* **9**, 1 (1983).
- [12] R. H. Goodman and R. Haberman, Kink-antikink collisions in the ϕ^4 equation: The n-bounce resonance and the separatrix map, *SIAM J. Appl. Dyn. Syst.* **4**, 1195 (2005).
- [13] R. H. Goodman and R. Haberman, Chaotic Scattering and the n-Bounce Resonance in Solitary-Wave Interactions, *Phys. Rev. Lett.* **98**, 104103 (2007).
- [14] H. Weigel, Kink-antikink scattering in ϕ^4 and ϕ^6 models, *J. Phys.: Conf. Ser.* **482**, 012045 (2014).
- [15] D. Bazeia, E. Belendryasova, and V. A. Gani, Scattering of kinks of the sinh-deformed ϕ^4 model, *Eur. Phys. J. C* **78**, 1 (2018).
- [16] M. Lizunova, J. Kager, S. de Lange, and J. van Wezel, Emergence of oscillons in kink-impurity interactions, *Journal of Physics A: Mathematical and Theoretical* (2021).
- [17] O. M. Braun and Y. S. Kivshar, Nonlinear dynamics of the Frenkel-Kontorova model with impurities, *Phys. Rev. B* **43**, 1060 (1991).
- [18] P. G. Kevrekidis and J. Cuevas-Maraver, *A Dynamical Perspective on the ϕ^4 Model* (Springer, Cham, Switzerland, 2019).
- [19] R. D. Yamaletdinov and Y. V. Pershin, in *Properties and Functionalization of Graphene*, edited by D. Tandabany and F. Hagelberg (Elsevier, 2021) [ArXiv:2011.13541](https://arxiv.org/abs/2011.13541).
- [20] J. C. Phillips, D. J. Hardy, J. D. Maia, J. E. Stone, J. V. Ribeiro, R. C. Bernardi, R. Buch, G. Fiorin, J. Hénin, and W. Jiang, *et al.* Scalable molecular dynamics on CPU and GPU architectures with NAMD, *J. Chem. Phys.* **153**, 044130 (2020).
- [21] W. Humphrey, A. Dalke, and K. Schulten, VMD – Visual Molecular Dynamics, *J. Mol. Graph.* **14**, 33 (1996).
- [22] NAMD and VMD were developed by the Theoretical and Computational Biophysics Group at the Beckman Institute for Advanced Science and Technology at the University of Illinois at Urbana-Champaign.
- [23] N. Foloppe and A. D. MacKerell Jr., All-atom empirical force field for nucleic acids: I. Parameter optimization based on small molecule and condensed phase macromolecular target data, *J. Comput. Chem.* **21**, 86 (2000).
- [24] A. D. MacKerell Jr. and N. K. Banavali, All-atom empirical force field for nucleic acids: II. Application to molecular dynamics simulations of DNA and RNA in solution, *J. Comput. Chem.* **21**, 105 (2000).
- [25] In simulations, the transformation between $((\alpha, +)$ antikinks, $(\alpha, -)$ kinks) and $((\alpha, +)$ antikinks, $(\alpha, -)$ kinks) can be achieved by application of a homogeneous force in the x direction.
- [26] Z. Shi, H. Lu, L. Zhang, R. Yang, Y. Wang, D. Liu, H. Guo, D. Shi, H. Gao, and E. Wang, *et al.* Studies of graphene-based nanoelectromechanical switches, *Nano Res.* **5**, 82 (2012).
- [27] J. Sun, W. Wang, M. Muruganathan, and H. Mizuta, Low pull-in voltage graphene electromechanical switch fabricated with a polymer sacrificial spacer, *Appl. Phys. Lett.* **105**, 033103 (2014).
- [28] J. Sun, M. Muruganathan, N. Kanetake, and H. Mizuta, Locally-actuated graphene-based nano-electro-mechanical switch, *Micromachines* **7**, 124 (2016).
- [29] M. E. Chen, M. M. Rojo, F. Lian, J. Koeln, A. Sood, S. M. Bohachuk, C. M. Neumann, S. G. Garrow, K. E. Goodson, A. G. Alleyne, and E. Pop, Graphene-based electromechanical thermal switches, *2D Mater.* **8**, 035055 (2021).
- [30] W. Bao, K. Myhro, Z. Zhao, Z. Chen, W. Jang, L. Jing, F. Miao, H. Zhang, C. Dames, and C. N. Lau, In situ observation of electrostatic and thermal manipulation of suspended graphene membranes, *Nano Lett.* **12**, 5470 (2012).
- [31] D. Yoon, Y.-W. Son, and H. Cheong, Negative thermal expansion coefficient of graphene measured by Raman spectroscopy, *Nano Lett.* **11**, 3227 (2011).
- [32] G. A. McQuade, A. S. Plaut, A. Usher, and J. Martin, The thermal expansion coefficient of monolayer, bilayer, and trilayer graphene derived from the strain induced by cooling to cryogenic temperatures, *Appl. Phys. Lett.* **118**, 203101 (2021).
- [33] International Roadmap for Devices and Systems (IRDSTM) 2021 Edition. <https://irds.ieee.org/editions/2021>, (2021).
- [34] M. Poot and H. S. van der Zant, Mechanical systems in the quantum regime, *Phys. Rep.* **511**, 273 (2012).